Transmission Eigenchannels and the Densities of States of Random Media

Matthieu Davy, Zhou Shi, Jing Wang, Xiaojun Cheng, and Azriel Z. Genack

Phys. Rev. Lett. **114**, 033901 — Published 23 January 2015

DOI: 10.1103/PhysRevLett.114.033901

Transmission eigenchannels and the densities of states of random media

Matthieu Davy,[1,2*] Zhou Shi,[1*] Jing Wang,[1] Xiaojun Cheng[1] and Azriel Z. Genack[1]

[1] *Department of Physics, Queens College of the City University of New York, Flushing, NY 11367, USA.*
[2] *Institut d'Electronique et de Télécommunications de Rennes, University of Rennes 1, Rennes 35042, France.*
[*] *These authors contributed equally to this work*

We show in microwave measurements and computer simulations that the contribution of each eigenchannel of the transmission matrix to the density of states (DOS) is the derivative with angular frequency of a composite phase shift. The accuracy of the measurement of the DOS determined from transmission eigenchannels is confirmed by the agreement with the DOS found from the decomposition of the field into modes. The distribution of the DOS, which underlies the Thouless number, is substantially broadened in the Anderson localization transition. We find a crossover from constant to exponential scaling of fluctuations of the DOS normalized by its average value. These results illuminate the relationships between scattering, stored energy and dynamics in complex media.

The transmission matrix (TM) is the basis of a powerful approach to quantum and classical wave propagation that is able to explain the statistics of conductance [1-7] and transmission [8] and prescribe the degree to which the transmitted wavefront can be manipulated [9-15]. It was introduced by Dorokhov to explain the scaling of electronic conductance in wires[1]. For a wire connected to perfectly conducting leads that support N propagating channels, and similarly for a waveguide between segments of empty waveguides, the $N \times N$ elements of thee TM, t, t_{ba}, are the field transmission coefficients through the sample between the incident channels a and outgoing channels b. The conductance in units of the quantum of conductance $G/(e^2/h)$ is equivalent to the classical transmittance T which can be expressed in terms of the transmission eigenvalues τ_n of the matrix product $tt^\dagger$, $T = \sum_{n=1}^{N} \tau_n$ [1, 6]. The probability distribution of these transmission eigenvalues determines the statistics of transmission [1-5, 8, 16].

For diffusive samples, the average of T over a random ensemble is given by $\langle T \rangle \equiv g = \xi / L$, where $\xi = N\ell$ is the localization length and ℓ is the transport mean free path.[17] For g>1, transport is diffusive and the flux transmitted through disordered samples in eigenchannels of transmission varies over a wide range with a small number of highly transmissive channels among a multitude of dark eigenchannels[1-5]. The transmittance is dominated by the approximately g "open" channels with transmission eigenvalues $\tau_n > 1/e$.

Recently, considerable attention has focused on the power of the TM to mold the flow of waves through random samples [14] and to modify the energy density inside the medium [18, 19]. The possibility of sharp focusing and enhanced transmission has been demonstrated for sound [20], elastic waves [21], light [9, 13, 22] and microwave radiation [12]. These phenomena have been described in terms of the transmission eigenvalues [9-13, 21], but static transmission parameters

cannot explain the dynamics of transmission or provide the DOS whose statistics control emission, absorption and wave localization and give the proclivity of a medium to emit radiation and store energy [23-33]. The crossover to wave localization reflects the changing character of the underlying modes, from extended to spatially peaked. This is characterized by the Thouless number δ, which is essentially the ratio of the typical linewidth to the spacing of classical modes or quantum energy levels [17, 34]. But the full statistics of modal overlap, reflected in δ have not been measured.

In this Letter, we show that the DOS can be determined from measurements of spectra of the TM. The contribution of each eigenchannel to the DOS is the derivative with angular frequency of a composite phase of the eigenchannel. Summing the contributions from all eigenchannels provides the first direct measurement of the DOS of a multiply scattering medium as a whole. The DOS determined from the eigenchannels is found to be in excellent agreement with the DOS found from a decomposition of the transmitted field into modes. The probability distribution of the DOS broadens substantially in the crossover to Anderson localization reflecting the increasing spectral isolation of long-lived localized modes. The eigenchannel phase derivative, which is equal to the delay time in transmission, increases with τ_n. When normalized by the average delay time, the eigenchannel delay time versus τ_n for diffusive samples of different length is found to fall on universal curve.

The DOS of a bounded open medium for classical waves is the density of quasi-normal modes or resonances of a region per unit angular frequency,[34]

$$\rho(\omega)=\frac{1}{\pi}\sum_n \frac{\Gamma_n/2}{(\Gamma_n/2)^2+(\omega-\omega_m)^2}. \qquad (1)$$

Here ω_n is the central frequency and Γ_n is the linewidth of the n^{th} mode. The integral over frequency of each mode in Eq. (1) is unity. Krein, Birman and Schwinger [24-26] have shown that the DOS may be expressed in terms of the scattering matrix S, $\rho(\omega)=-i\frac{1}{2\pi}TrS^{\dagger}dS/d\omega$, where $-iS^{\dagger}dS/d\omega$ is the Wigner-Smith delay-time matrix whose trace is equal to the sum of scattering times in all $2N$ channels linked to the scattering region [27, 28]. This is proportional to the integral of the energy stored within the medium for unit incident flux in each channel, $\rho(\omega)\propto\sum_{\alpha}^{2N}\int_V I_{\alpha}(r,\omega)dV$ [28, 30]. The difficulty of carrying out measurements over all possible scattering channels has so far precluded a determination of the DOS based on the scattering matrix. However, the calculations of Brandbydge and Tsukada [29] of the local DOS of electrons based on the scattering matrix show that the DOS can be determined from measurements of the TM. The DOS can be obtained from the summation of the derivative of composite phase of the transmission eigenchannels with angular frequency. The phase derivative of the n^{th} transmission eigenchannel, $\frac{d\theta_n}{d\omega}=\frac{1}{i}(\mathbf{u}_n^{*}\frac{d\mathbf{u}_n}{d\omega}-\mathbf{v}_n^{*}\frac{d\mathbf{v}_n}{d\omega})$, where $\mathbf{v_n}$ and $\mathbf{u_n}$ are n^{th} columns of the unitary matrices V and U, may be obtained from the singular value decomposition of the TM, $t=U\Lambda V^{\dagger}$ [35]. Λ is a diagonal matrix with elements $\sqrt{\tau_n}$. The DOS is then

$$\rho(\omega)=\frac{1}{\pi}\sum_{n=1}^{N}\frac{d\theta_n}{d\omega}. \quad (2)$$

Each term in the sum is the contribution of a single eigenchannel to the DOS, the eigenchannel density of states (EDOS).

This relation is an extension to multichannel systems of the equality between the DOS and the transmission delay time in 1D systems [31]. The eigenchannel phase derivative $d\theta_n/d\omega$ corresponds to the delay time $\Delta t_n(\omega)$ of energy for a transmitted pulse composed of a superposition of waves in the n^{th} eigenchannel centered at ω in the limit of vanishing bandwidth [35].

Measurements of the TM for which the impact of absorption is removed are carried out in a copper waveguide containing randomly positioned alumina spheres [10, 16, 35, 36]. The empty waveguide supports $N\sim 66$ modes for diffusive waves and $N\sim 30$ for localized waves. Measurements are made for linearly polarized horizontal and vertical components of the field over the front and back surfaces of the waveguide by translating and rotating wire antennas on a square grid. The TM is computed using $N/2$ points for each polarization for diffusive wave. For localized waves, the measurements reported here are made for only a single polarization. The measurement of the TM on a grid for a single polarization is incomplete [11, 13], but we find that the statistics of the TM are well represented by the measured TM provided that the measured size of the TM, N', is much greater than the value of dimensionless conductance g in the sample [11, 16]. New configurations are obtained by briefly rotating and vibrating the sample tube. For diffusive waves, the TM was measured for three sample lengths, L=23, 40 and 61 cm, while for localized waves, measurements are reported here for samples of length L= 40 cm.

Microwave spectra of τ_n and $d\theta_n/d\omega$ for a single random configuration drawn from an ensemble of diffusive samples with g=6.9 and localized samples with g=0.37 are shown in Fig. 1. In Fig. 2 we compare the DOS determined from the sum in Eq. (1) of contributions from all modes to the DOS given by the sum over eigenchannels in Eq. (2). The comparison is made for waves in the crossover to Anderson localization for which the degree of modal overlap is appreciable but still small enough that the full set of mode central frequencies ω_n and linewidths Γ_n and so the contribution to the DOS for each mode can be accurately determined from a decomposition of field spectra [37]. The DOS found from the modal decomposition involves the analysis of the entire field spectrum and modes can be found from measurements of the TM as well as from measurements of field spectra within the interior of the sample [35], from which it is impossible to find the transmission eigenchannels. In contrast, the analysis of the transmission eigenchannels requires only the TM at two slightly shifted frequencies so that the derivative of the phase can be found. Thus the DOS determined from an analysis of modes and channels is independent. A plot of the spectrum of the individual modes corresponding to the terms in Eq. (1) is shown in Fig. 2a. Good agreement is found in Fig. 2b between the sums of the contributions to the DOS of all eigenchannels and of all modes determined from the TM and from spectra of the field inside the sample. The analysis of the TM can thus be used to find the DOS in samples with strong modal overlap for modal analysis is not possible.

The degree of overlap of the modes of the medium is a fundamental indicator of the nature of wave propagation. This is encapsulated in the Thouless number, which is essentially the average of the ratio of the spectral width and spacing of modes [17, 37]. A more comprehensive representation of the nature of modal overlap in random systems would be the probability distribution of the relative DOS, $\rho(\omega)/<\rho(\omega)>$, which can be constructed from spectra of $\sum_{n=1}^{N} d\theta_n / d\omega$. The probability distributions $P(\sum_{n=1}^{N} \frac{d\theta_n}{d\omega} / \langle \sum_{n=1}^{N} \frac{d\theta_n}{d\omega} \rangle)$ measured for ensembles of samples with L_{eff}/ξ ranging from 0.14 to 2 are shown in Fig. 3a. The effective sample length [38] is $L_{eff} = L + 2z_b$ with intensity extrapolation lengths beyond the sample reflecting internal reflection of z_b=6 cm for localized waves and 13 cm for diffusive waves [10]. The distributions are seen to broaden with increasing sample length *L,* particularly beyond the crossover to localization at $L/\xi = 1$ when distinct peaks begin to emerge in the spectrum of the DOS. For $L_{eff}/\xi = 2.08$, the probability distribution of the DOS, $P(\rho)$, is seen in Fig. 3b to exhibit an algebraic tail as $1/\rho^{4.8}$ in agreement with simulations for this sample [35]. For $L >> \xi$, the tail of the time delay distribution for transmitted waves in a random 1D sample, which is the same as the DOS, is $P(\rho) \propto 1/\rho^2$ [39, 40]. The probability distribution of transmittance, $P(T)$, for quasi-1D samples is found to approach the log-normal distribution predicted for $L >> \xi$ in 1D samples [41] only when the participation number of transmission eigenchannels[12], $M \equiv (\sum_{n=1}^{N} \tau_n)^2 / \sum_{n=1}^{N} \tau_n^2$ is very close to unity. $P(T)$ for the sample with L_{eff}/ξ=2.08 is a one-sided log-normal distribution [16] and we would not expect $P(\rho)$ to reach its asymptotic form for $L/\xi >> 1$.

We carry out two-dimensional numerical simulations using the recursive Green's function method [42] to explore the fluctuations of the DOS as well as to determine the impact of an incomplete measurement of the TM on estimates of the DOS. Spectra of $d\theta_n / d\omega$ for a diffusive sample with $L/\xi = 0.69$ and N=33 in which fluctuations in spectra of the EDOS are still appreciable are shown in Fig. 4a. $d\theta_n / d\omega$ is seen to coincide with normalized spectra of the integral of the energy density over the sample volume for a transmission eigenchannel $\int_V I_n(r,\omega) dV$ [35], confirming that $d\theta_n / d\omega$ is the contribution of the n^{th} eigenchannel to the DOS, the EDOS. However, it is difficult to excite and detect all channels and the measured TM for diffusive waves is typically incomplete. $(d\theta_n / d\omega)/\pi$ is then no longer equal to the EDOS and its sum does not give the DOS. Similarly, it is not possible to construct a fully transmitted incident wave when the TM is not complete [11]. We estimate that the best agreement between measurements of $\langle d\theta_n / d\omega \rangle$ and simulations of $\langle d\theta_n / d\omega \rangle$ shown in Fig. 5b occurs when we construct the simulated TM using a fraction $N'/N = 0.7$ of the channels of the system. The best agreement between measurements and calculations of the probability distribution of transmission eigenvalues is also obtained for $N'/N = 0.7$ [35].

In Fig. 4a slight differences between spectra of the sum of $d\theta_n / d\omega$ for a complete TM and for a sample with $N'/N = 0.7$ are observed. The probability distributions $P(\sum_{n=1}^{N} d\theta_n / d\omega)$ shown in

Fig. 4b are quite similar when $N' >> M$. Significant deviations arise, however, for diffusive samples in which M is comparable to or larger than N'. The number of measured channels is then insufficient to accurately reflect the nature of transport.

In Fig. 4b and 4c, we show the results of simulation of the scaling of the variance of $\rho(\omega)/<\rho(\omega)>$ for samples with N=16 and N=33 together with the result obtained from the distribution shown in Fig. 3 for $L_{eff}/\xi = 2.07$. In this case $N' >> M$. Measurements are seen to be in good agreement with simulations. The variance for diffusive waves, for $L/\xi < 1$, is flat with a value of ~ 0.003 for N=33 and ~ 0.007 for N=16. Rigidity in the spectrum of the central frequencies of electromagnetic modes when many modes fall within the mode linewidth [43] is likely the origin of the constant value of the variance of $\rho(\omega)/<\rho(\omega)>$ for each value of N. For deeply localized waves, mode spacing typically exceeds the linewidth so that fluctuations of the DOS increases rapidly with L/ξ as modal linewidths fall. The variance of $\rho(\omega)/<\rho(\omega)>$ is seen in Fig. 4c to increases exponentially as $e^{1.6L/\xi}$. Thus fluctuations of the DOS provide an experimental measure of L/ξ and of the degree of modal overlap for both diffusive and localized waves [43].

The variation of the transmission delay time with the transmission eigenvalue in diffusive samples is shown in Fig. 5a. $\langle d\theta_n / d\omega \rangle$ increases with τ_n and sample length so that delay times are lengthened in coherent eigenchannels with high transmission. When normalized by the ensemble average of the photon delay time, which is the average of the single channel delay time between channels a and b weighted by the transmitted intensity $|t_{ba}|^2$, $\langle d\varphi / d\omega \rangle = <\sum_{ab} |t_{ab}|^2 \, d\varphi_{ab} / d\omega> / <\sum_{ab} |t_{ab}|^2>$, the measurements collapse to a single curve (Fig. 5b). This is confirmed in simulations as shown in Fig. 5c. The constant ratio of the delay time $\langle d\theta_n / d\omega \rangle$ averaged over eigenchannels of fixed τ_n, to the average delay time together with the scaling of $\langle d\varphi / d\omega \rangle$ as L^2 for diffusive waves [44] indicates that the EDOS for a given value of τ_n scales as L^2, as seen in Fig. 5d for τ_n =0.1 and 1. Though the EDOS scales as L^2, the DOS is seen in Fig 5d to scale as L, as expected, since the number of open channels with $\tau_n > 1/e$ is proportional to $g = \xi / L$ [1, 2], falls inversely with L.

We have shown that it is possible to measure the dynamics and stored energy in addition to the transmission of each transmission eigenchannel. This makes it possible to measure the DOS as well as the transmittance for both diffusive and localized waves. Fluctuations in the DOS can provide a rich picture of the changing nature of transport in the Anderson localization transition. The cumulant correlation function with frequency shift of the DOS normalized to its average may yield the statistics of the spacing of energy levels and the probability of return of scattered particle of the wave to a coherence volume within the sample vs. time delay. The wave becomes localized when the probability of return integrated over time equals unity [43, 45]. Selective excitation of highly-transmissive, long-lived eigenchannels can enhance energy collection and lower the threshold of random lasers.

We thank Evgeni Gurevich for stimulating discussion on the scattering matrix and Arthur Goetschy and A. Douglas Stone for providing the simulation code to calculate the transmission matrix through a two dimensional disordered waveguide. The research was supported by the National Science Foundation (DMR-1207446) and by the Direction Générale de l'Armement (DGA).

References

[1] O. N. Dorokhov, Solid State Commun. **51**, 381 (1984).
[2] Y. Imry, Euro. Phys. Lett. **1**, 249 (1986).
[3] P. Mello, P. Pereyra, and N. Kumar, Ann. Phys. (N. Y.) **181**, 290 (1988).
[4] J. B. Pendry, A. MacKinnon, and P. J. Roberts, Proc. R. Soc. London A **437**, 67 (1992).
[5] C. W. J. Beenakker, Rev. Mod. Phys. **69**, 731 (1997).
[6] D. S. Fisher and P. A. Lee, Phys. Rev. B **23**, 6851 (1981).
[7] R. A. Webb, S. Washburn, C. P. Umbach, and R. B. Laibowitz, Phys. Rev. Lett. **54**, 2696 (1985).
[8] M. C. W. van Rossum and T. M. Nieuwenhuizen, Rev. Mod. Phys. **71**, 313 (1999).
[9] I. M. Vellekoop and A. P. Mosk, Phys. Rev. Lett. **101**, 120601 (2008).
[10] Z. Shi and A. Z. Genack, Phys. Rev. Lett. **108**, 043901 (2012).
[11] A. Goetschy and A. D. Stone, Phys. Rev. Lett. **111**, 063901 (2013).
[12] M. Davy, Z. Shi, J. Wang, and A. Z. Genack, Opt. Express **21**, 10367 (2013).
[13] H. Yu, T. R. Hillman, W. Choi, J. O. Lee, M. S. Feld, R. R. Dasari, and Y. K. Park, Phys. Rev. Lett. **111**, 153902 (2013).
[14] A. P. Mosk, A. Lagendijk, G. Lerosey, and M. Fink, Nature Photon. **6**, 283 (2012).
[15] T. Chaigne, O. Katz, A. C. Boccara, M. Fink, E. Bossy, and S. Gigan, Nat. Photon. **8**, 58 (2014).
[16] Z. Shi, J. Wang, and A. Z. Genack, Proc. Natl. Acad. Sci., 201319704 (2014).
[17] D. J. Thouless, Phys. Rev. Lett. **39**, 1167 (1977).
[18] S. Rotter, P. Ambichl, and F. Libisch, Phys. Rev. Lett. **106**, 120602 (2011).
[19] W. Choi, A. P. Mosk, Q. H. Park, and W. Choi, Phys. Rev. B **83**, 134207 (2011).
[20] A. Derode, P. Roux, and M. Fink, Phys. Rev. Lett. **75**, 4206 (1995).
[21] B. Gérardin, J. Laurent, A. Derode, C. Prada, and A. Aubry, Phys. Rev. Lett. **113**, 173901 (2014).
[22] S. M. Popoff, A. Goetschy, S. F. Liew, A. D. Stone, and H. Cao, Phys. Rev. Lett. **112**, 133903 (2014).
[23] E. Purcell, Phys. Rev. **69**, 681 (1946).
[24] M. G. Krein, Dokl Akad Nauk SSSR **144**, 475 (1962).
[25] M. S. Birman and D. R. Yafaev, Algebra i Analiz **4**, 1 (1992).
[26] J. Schwinger, Phys. Rev. **82**, 664 (1951).
[27] E. P. Wigner, Phys. Rev. **98**, 145 (1955).
[28] F. T. Smith, Phys. Rev. **118**, 349 (1960).
[29] M. Brandbyge and M. Tsukada, Phys. Rev. B **57**, R15088 (1998).
[30] G. Iannaccone, Phys. Rev. B **51**, 4727 (1995).
[31] Y. Avishai and Y. B. Band, Phys. Rev. B **32**, 2674 (1985).
[32] T. Kottos and U. Smilansky, J. Phys. A: Math. Gen. **36**, 3501 (2003).
[33] Y. V. Fyodorov and H.-J. Sommers, J. Math. Phys. **38**, 1918 (1997).

[34] G. Breit and E. Wigner, Phys. Rev. **49**, 519 (1936).
[35] See Supplemental Material [url], which includes Refs. [10,24-26,29,32,39,42].
[36] A. A. Chabanov, M. Stoytchev, and A. Z. Genack, Nature **404**, 850 (2000).
[37] J. Wang and A. Z. Genack, Nature **471**, 345 (2011).
[38] A. Lagendijk, R. Vreeker, and P. De Vries, Phys. Lett. A **136**, 81 (1989).
[39] C. Texier and A. Comtet, Phys. Rev. Lett. **82**, 4220 (1999).
[40] A. Ossipov, T. Kottos, and T. Geisel, Phys. Rev. B **61**, 11411 (2000).
[41] P. W. Anderson, D. J. Thouless, E. Abrahams, and D. S. Fisher, Phys. Rev. B **22**, 3519 (1980).
[42] H. U. Baranger, D. P. DiVincenzo, R. A. Jalabert, and A. D. Stone, Phys. Rev. B **44**, 10637 (1991).
[43] B. Altshuler and B. Shklovskii, Sov. Phys. JETP **64**, 127 (1986).
[44] R. Landauer and M. Buttiker, Phys. Rev. B **36**, 6255 (1987).
[45] N. Argaman, Y. Imry, and U. Smilansky, Phys. Rev. B **47**, 4440 (1993).

[46] [first reference in Supplemental Material not already in Letter] M. G. Krein, Sov. Math. Dokl **3**, 707 (1962).
[47] M. Š. Birman and M. G. Kreĭn, in *Outlines Joint Sympos. Partial Differential Equations (Novosibirsk, 1963)*1963), pp. 39.
[48] J. Jauch, K. Sinha, and B. Misra, Helv. Phys. Acta **45** (1972).
[49] R. G. Newton, *Scattering theory of waves and particles* (DoverPublications. com, 1982).
[50] P. Sebbah, O. Legrand, B. A. van Tiggelen, and A. Z. Genack, Phys. Rev. E **56**, 3619 (1997).
[51] P. Sebbah, O. Legrand, and A. Z. Genack, Phys. Rev. E **59**, 2406 (1999).
[52] A. Z. Genack, P. Sebbah, M. Stoytchev, and B. A. van Tiggelen, Phys. Rev. Lett. **82**, 715 (1999).
[53] [last reference in Supplemental Material not already in Letter] A. Goetschy and A. D. Stone, Phys. Rev. Lett. **111**, 063901 (2013).

FIGURES

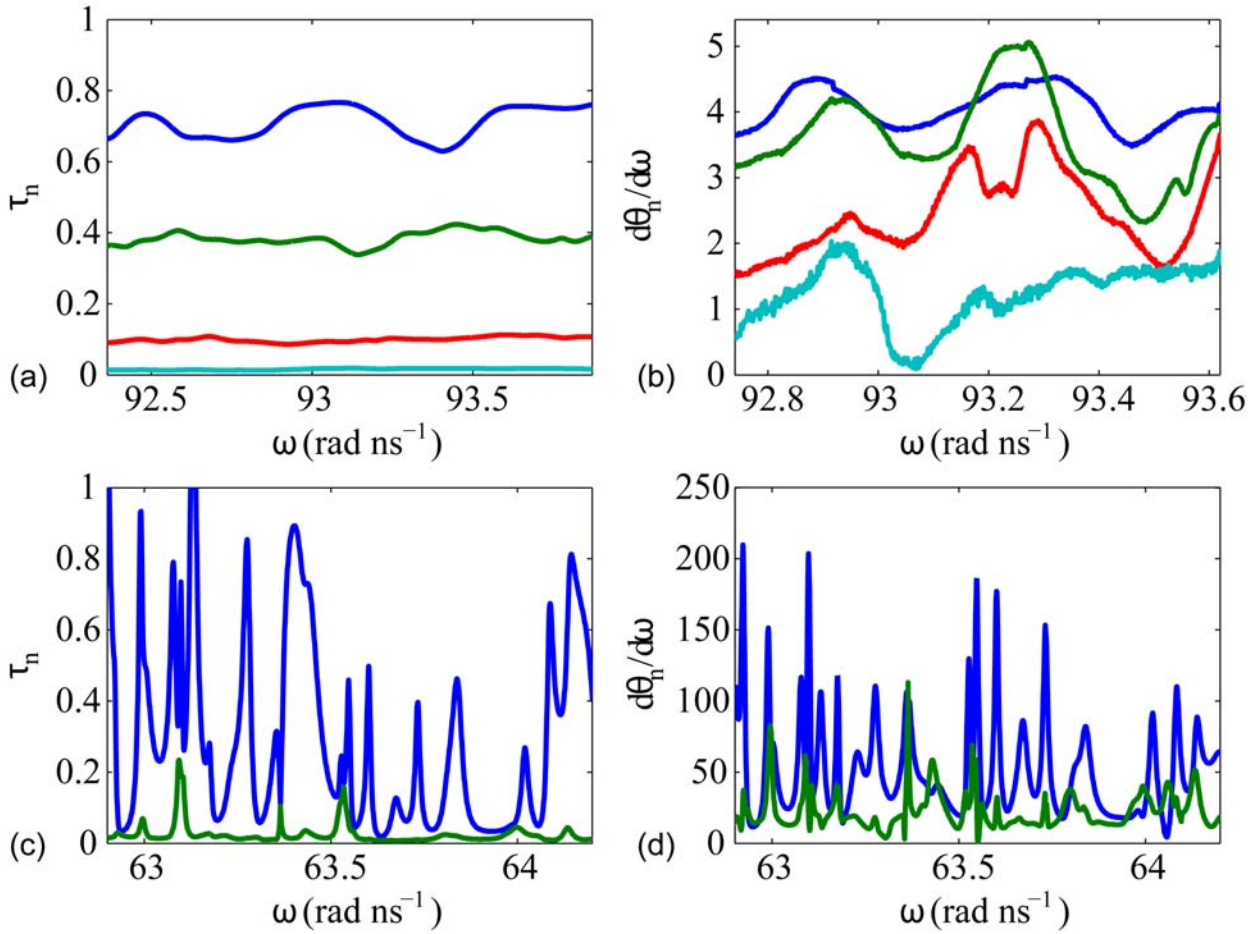

FIG. 1 (color online). Spectra of τ_n (a,c) and spectra of $\left(d\theta_n / d\omega\right)$ (b,d) for eigenchannels n=1,5,15,25 for diffusive waves of sample length L=23 cm with g=6.9 (a,b), and n=1,2 for localized waves of length L=40 cm and g=0.37 (c,d).

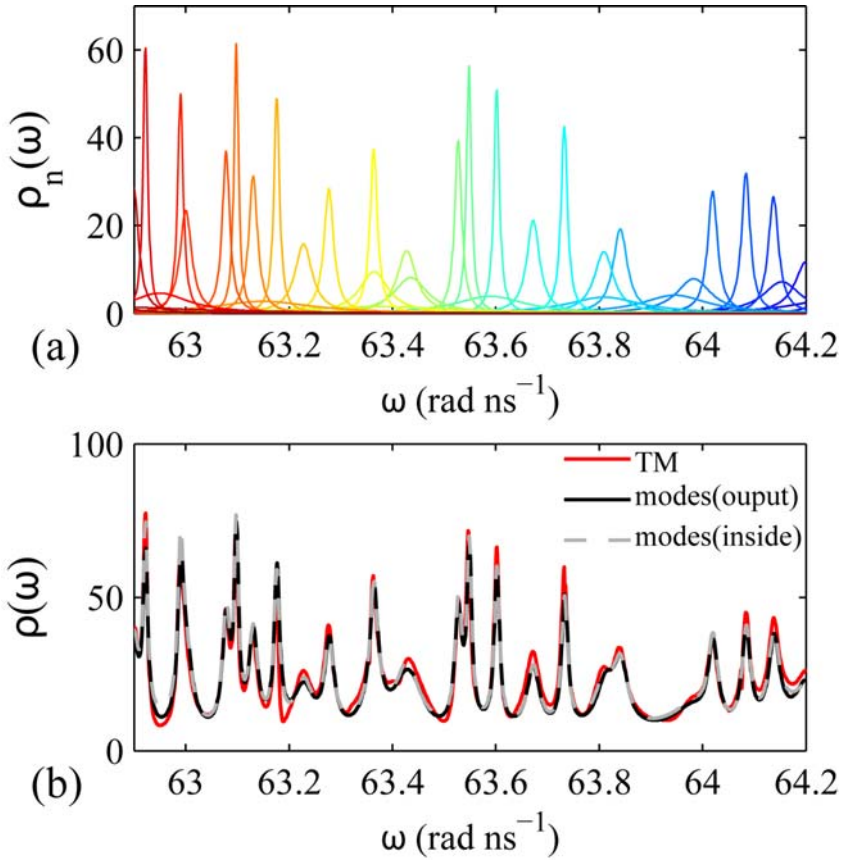

FIG. 2 (color online). (a) Contributions of the individual modes in Eq. (1) to the DOS. (b) Comparison of the DOS determined from the TM (red curve) by summing spectra of $\left(d\theta_n / d\omega\right)$ and modes found from spectra of the field at the output (black curve) and from spectra of the field inside the sample (grey dotted curve).

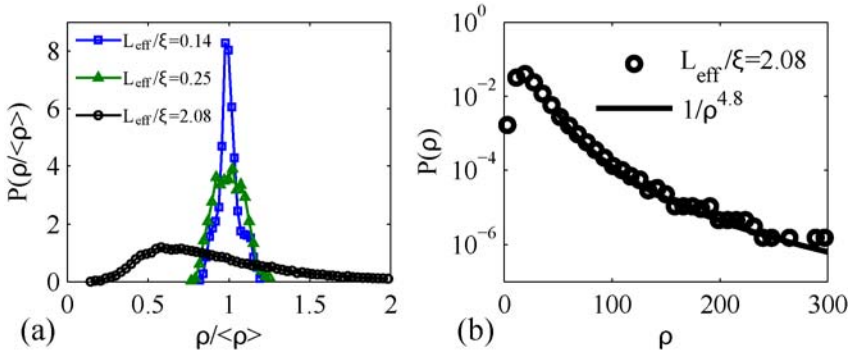

FIG. 3 (color online). (a) Measurement of probability distribution of the DOS normalized by its average value determined from the sum of $d\theta_n / d\omega$ for L_{eff}/ξ=0.14 (blue squares), L_{eff}/ξ=0.25 (green triangles) and L_{eff}/ξ=2.08 (black circles). (b) Probability distribution of the DOS for L_{eff}/ξ=2.08 in a semilog scale. The black line is a fit of the tail as $1/\rho^{4.8}$.

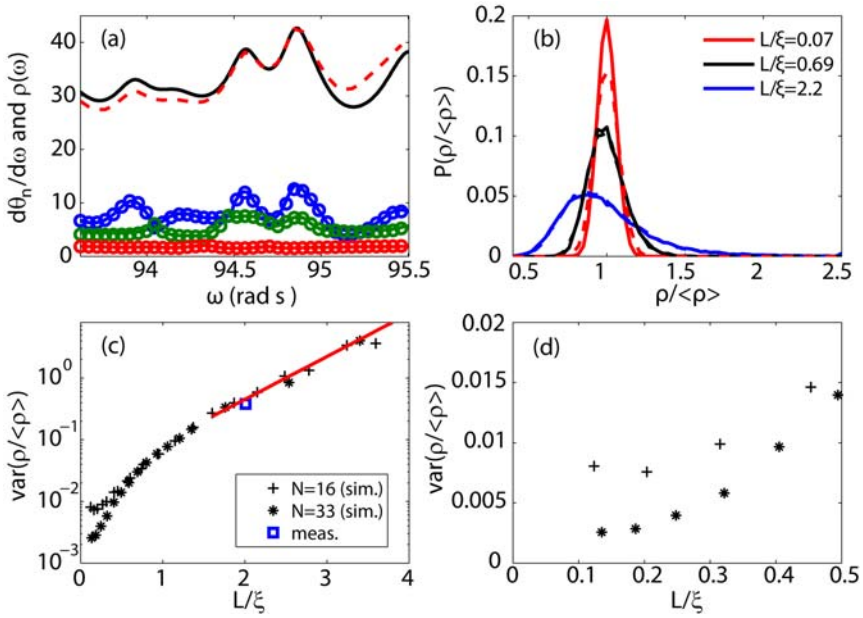

FIG. 4 (color online). (a) Spectra of $d\theta_n / d\omega$ (full curves) and the normalized integral of the energy density $I_n(z)$ inside the sample (circles), for eigenchannels with $\tau = 0.8$ (blue line), $\tau = 0.5$ (green line), $\tau = 0.01$ (red line) for N=33 and L/ξ=0.69. The black curve is $\rho(\omega)$. The red dashed curve is $\sum_{n=1}^{N'} d\theta_n / d\omega$ for an incomplete measurement of the TM with N'/N=0.7. (b) Probability distribution $P(\rho/<\rho>)$ for $L/\xi = 0.07$ (red line), $L/\xi = 0.69$ (black line) and $L/\xi = 2.2$ (blue line). The corresponding dashed curves are $P(\sum_{n=1}^{N'} d\theta_n / d\omega / < \sum_{n=1}^{N'} d\theta_n / d\omega >)$ with $N'/N = 0.7$. (c) Variation of the variance of the normalized DOS, $\mathrm{var}(\rho/<\rho>)$, as a function of L/ξ in simulation with N=16 (black crosses) and N=33 (black stars) and in measurements (squares). The red line is an exponential fit of the data for localized waves, $L/\xi > 1$. The results are obtained from 5000 simulations of samples with the same length but different degree of disorder. (d) Linear plot of $\mathrm{var}(\rho/<\rho>)$ for diffusive waves.

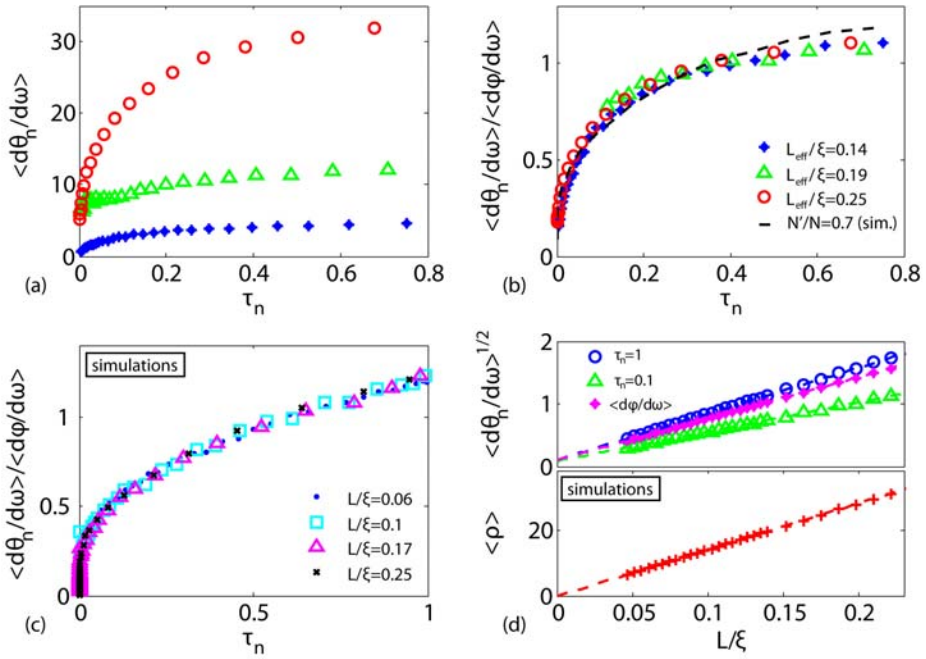

FIG. 5 (color online). (a) Averages of measured $\langle d\theta_n / d\omega\rangle$ and (b) $\langle d\theta_n / d\omega\rangle / \langle d\varphi / d\omega\rangle$, vs. τ_n for L=61cm (red circles), L=40 cm (green triangles) and L=23 cm (blue filled circles). The black curve is obtained from simulations in which $N'/N = 0.7$. (c) simulations for the complete TM of $\langle d\theta_n / d\omega\rangle / \langle d\varphi / d\omega\rangle$ with $L/\xi = 0.06$ (blue dots), $L/\xi = 0.1$ (cyan squares), $L/\xi = 0.17$ (magenta triangles) and $L/\xi = 0.25$ (black crosses). (d) Scaling of $\sqrt{\langle d\theta_n / d\omega\rangle}$ for eigenchannels with $\tau = 1$ (blue dots) and $\tau = 0.1$ (blue triangles), of $\sqrt{\langle d\varphi / d\omega\rangle}$ (blue stars), and of $<\rho>$ (red crosses).